



<b>Publication Year</b>	2015
<b>Acceptance in OA @INAF</b>	2020-03-03T16:20:47Z
<b>Title</b>	Matching the Evolution of the Stellar Mass Function Using Log-Normal Star Formation Histories
<b>Authors</b>	Abramson, Louis E.; Gladders, Michael D.; Dressler, Alan; Oemler, Augustus, Jr.; POGGIANTI, Bianca Maria; et al.
<b>DOI</b>	10.1088/2041-8205/801/1/L12
<b>Handle</b>	<a href="http://hdl.handle.net/20.500.12386/23090">http://hdl.handle.net/20.500.12386/23090</a>
<b>Journal</b>	THE ASTROPHYSICAL JOURNAL
<b>Number</b>	801

## MATCHING THE EVOLUTION OF THE STELLAR MASS FUNCTION USING LOG-NORMAL STAR FORMATION HISTORIES

LOUIS E. ABRAMSON<sup>1</sup>, MICHAEL D. GLADDERS<sup>1</sup>, ALAN DRESSLER<sup>2</sup>, AUGUSTUS OEMLER, JR.<sup>2</sup>,  
 BIANCA POGGIANTI<sup>3</sup>, AND BENEDETTA VULCANI<sup>4</sup>

<sup>1</sup>Department of Astronomy & Astrophysics and Kavli Institute for Cosmological Physics, The University of Chicago,  
 5640 South Ellis Avenue, Chicago, IL 60637, USA; [labramson@uchicago.edu](mailto:labramson@uchicago.edu)

<sup>2</sup>The Observatories of the Carnegie Institution for Science, 813 Santa Barbara Street, Pasadena, CA 91101, USA

<sup>3</sup>INAF-Osservatorio Astronomico di Padova, Vicolo Osservatorio 5, I-35122 Padova, Italy

<sup>4</sup>Kavli Institute for the Physics and Mathematics of the Universe (WPI), Todai Institutes for Advanced Study,  
 University of Tokyo, Kashiwa 277-8582, Japan

*Received 2014 November 6; accepted 2015 January 14; published 2015 March 2*

### ABSTRACT

We show that a model consisting of individual, log-normal star formation histories for a volume-limited sample of  $z \approx 0$  galaxies reproduces the evolution of the total and quiescent stellar mass functions at  $z \lesssim 2.5$  and stellar masses  $M_* \geq 10^{10} M_\odot$ . This model has previously been shown to reproduce the star formation rate/stellar mass relation (SFR– $M_*$ ) over the same interval, is fully consistent with the observed evolution of the cosmic SFR density at  $z \leq 8$ , and entails no explicit “quenching” prescription. We interpret these results/features in the context of other models demonstrating a similar ability to reproduce the evolution of (1) the cosmic SFR density, (2) the total/quiescent stellar mass functions, and (3) the SFR– $M_*$  relation, proposing that the key difference between modeling approaches is the extent to which they stress/address diversity in the (star-forming) galaxy population. Finally, we suggest that observations revealing the timescale associated with dispersion in SFR( $M_*$ ) will help establish which models are the most relevant to galaxy evolution.

*Key words:* galaxies: evolution – galaxies: luminosity function, mass function – galaxies: star formation

### 1. INTRODUCTION

Three measurements have emerged as central to the study of galaxy star formation histories (SFHs):

- (1) the cosmic star formation rate density (SFRD; see Madau & Dickinson 2014 and references therein);
- (2) the stellar mass function,  $\Phi(M_*)$ , for star-forming ( $\Phi_{\text{SF}}$ ) and quiescent ( $\Phi_{\text{Q}}$ ) galaxies (e.g., Tomczak et al. 2014);
- (3) the SFR– $M_*$  relation, or SF “main Sequence” (SFMS; e.g., Brinchmann et al. 2004; Noeske et al. 2007; Salmon et al. 2014).

Any viable theory of galaxy evolution must reproduce these observations.

These “pillars” rest on each other physically:

$$\text{SFRD}(t) = \int \Phi_{\text{SF}}(M_*, t) \langle \text{SFR}(M_*, t) \rangle dM_*. \quad (1)$$

Cosmic SFRD evolution depends explicitly on the evolution of the (star-forming) stellar mass function and the SFMS (i.e.,  $\langle \text{SFR}(M_*, t) \rangle$ ). Depending on the modeling approach, one of these phenomena can emerge naturally if the other two are reproduced, but all serve as checks/constraints regardless of technique. That is, even if a model describes a plausible evolutionary scenario for  $\Phi$  based on the SFMS, it is not an accurate scenario unless the correct SFRD( $t$ ) emerges as a consequence.

In Gladders et al. (2013, hereafter G13), noting that the cosmic SFRD( $t$ ) is remarkably log-normal in shape, we posited that this analytic form might also describe the SFHs of individual galaxies. We developed a model comprised of log-normal SFHs for a volume-complete sample of  $z \approx 0$  galaxies ( $M_* \geq 10^{10} M_\odot$ , any sSFR) by jointly fitting their

observed  $M_*$ , SFR values and the SFRD at  $z \leq 8$ . While SFRD( $t$ ) was thus matched by construction, we showed that the model also reproduced observed sSFR distributions at  $0.2 \leq z \leq 1$ , and the SFMS at  $z \sim 2$  when those distributions were reincorporated as constraints. We did not, however, examine the model’s implications for the stellar mass function.

Here, we complete the analysis by comparing G13 model predictions to the observed evolution of  $\Phi$  and  $\Phi_{\text{Q}}$ , showing that the data are reproduced with remarkable fidelity. By doing so, we demonstrate that a purely “dispersion-based” approach—which addresses diversity in the galaxy population—can match key ensemble metrics of galaxy evolution previously modeled using mean, statistical relations (e.g., Peng et al. 2010; Behroozi et al. 2013). We close by describing ways to elucidate how well the SFHs of real galaxies fit into these paradigms.

### 2. LOG-NORMAL STAR FORMATION HISTORIES

A detailed account of the extraction of SFHs can be found in G13, but we review some critical aspects below.

#### 2.1. Modeling

The fitting procedure mentioned above found the best log-normal SFH parameters (Equation (2)) for 2094 galaxies at  $\langle z \rangle \simeq 0.07$  based on how well the ensemble of such histories matched the observed SFRD at ( $z \leq 8$ ). Explicitly, the shape of the SFH of the  $i$ th galaxy in a comoving volume  $V$ —drawn from the Sloan Digital Sky Survey (York et al. 2000) and the Padova Millennium Galaxy and Group Catalog (Calvi

et al. 2011)—was

$$\text{SFR}(t)_i \propto \frac{1}{\sqrt{2\pi\tau_i^2}} \frac{\exp\left[-\frac{(\ln t - T_{0,i})^2}{2\tau_i^2}\right]}{t}, \quad (2)$$

where  $(T_0, \tau)$  are the peak-time and width of each SFH in  $\ln(t)$ , respectively. The fitting determined the best values for these parameters such that (1) individual SFHs—normalized to the appropriate  $M_*$ —produced a galaxy’s observed SFR at  $z = z_{\text{obs}}$ , and (2) the ensemble of SFHs summed to the observed SFRD( $t$ ):

$$\sum_{i=1}^{N_{\text{gals}}} \text{SFR}(t)_i = V \cdot \text{SFRD}(t), \quad (3)$$

for all  $t$  spanned by the SFRD data (Cucciati et al. 2012).

This approach is extremely flexible, entails no assumptions about the data, and is highly predictive in principle: any SFH-related observable (e.g., colors) could be derived for any redshift spanned by the SFRD data. Of course, these virtues require imposing a form to  $\text{SFR}(t)$ .

For our final **G13** model—upon which this paper is based—we included the zeropoint of the SFMS and its *dispersion* collapsed across  $M_*$  as additional constraints at various  $z \lesssim 1$ . Thus, the normalization and spread of the SFHs were constrained at  $z \lesssim 1$ , but not  $\text{SFR}(M_*)$  itself; i.e., no  $M_* \mapsto \text{SFR}$  mapping was imposed anywhere except implicitly through the  $z \approx 0$  input data. Likewise, the  $M_*$  distribution (i.e.,  $\Phi$ ) was set only implicitly by these data (complete to  $M_* = 10^{10} M_\odot$ ); it was never used as an explicit fitting constraint.

## 2.2. Quiescent Fractions

At any epoch constrained by a sSFR distribution, the **G13** procedure ensured only that the total fraction of quiescent SFHs matched the total observed fraction of quiescent galaxies. “Quiescent” was defined as  $\log \text{sSFR}(M_*, t) < [\langle \log \text{sSFR}(M_*, t) \rangle - 0.6 \text{ dex}]$ ; i.e., about  $1.5\sigma$  below the mean SFMS relation. Model SFHs could take any value below this threshold.

While the quiescent definition was thus mass-dependent, the fitter considered only the total number of SFHs meeting it, so the resulting model  $M_*$  distributions were unconstrained. This approach affects the normalization, but not the *shape* of  $\Phi_Q$ . No aspect of our modeling guarantees that the detailed evolution of  $\Phi$  or  $\Phi_Q$  will be reproduced, so comparisons to these data are valid tests of our log-normal SFH parametrization.

## 3. RESULTS

### 3.1. Predictions for the Evolution of $\Phi$ and $\Phi_Q$

We plot  $\Phi$  and  $\Phi_Q$  as measured by Tomczak et al. (2014) and Muzzin et al. (2013) across  $0.5 \lesssim z \lesssim 2.5$  and overlay our model predictions in Figure 1. Model uncertainties derive from marginalizing over galaxy merger histories (see **G13** for details), locations within a redshift bin, and random  $M_*$  errors of 0.1 dex (consistent with typical values; e.g., Kauffmann et al. 2003). Solid lines show results if mergers are neglected.

Two points are key. The first is that the model reproduces the evolution of the shape and normalization of  $\Phi$  very accurately, especially when considering uncertainties in the data and

merger prescription. Though “informed” only of the total  $\dot{M}_*$  evolution of the universe (via  $\text{SFRD}(t)$ ), this result shows that the model put that mass in the correct place ( $M_*$ -bin) at the correct time. This suggests that the log-normal parametrization is in fact a good approximation of real galaxy SFHs, at least at the mass-bin level.

The second point is that the model reproduces the shape of  $\Phi_Q$ , especially the turnover at  $M_* < M_Q^*$  not exhibited by  $\Phi$  or  $\Phi_{\text{SF}}$  (e.g., Ball et al. 2006; Moustakas et al. 2013; Muzzin et al. 2013; Tomczak et al. 2014). Hence, even though the model contains *no* explicit quenching prescription, it produces the correct evolution from the star-forming to quiescent populations (defined as a cut in sSFR; Section 2.2) as a function of  $M_*$  and time. This suggests that the model SFHs for quiescent galaxies are both accurate absolutely—for a given mass-bin—and appropriately divergent from those of equal-mass star-forming contemporaries (Figure 2). However, as discussed in Section 3.2, “divergent” in this context does not mean “subject to additional physics.”

No data from the comparison observations was used at any point except to normalize the total mass functions (gray curves to black points) in the first two panels (top-left). All other panels show epochs where the **G13** model was constrained only by  $\text{SFRD}(t)$ , i.e., where the model was sensitive only to a number—the integral of  $\Phi_Q$  or  $\Phi_{\text{SF}}$  ( $= \Phi - \Phi_Q$ ; see Equation (1)). Thus, the fact that the mass *distributions* resemble the data at better than the factor of 2 level at all  $M_*$  is rather remarkable. Indeed, this is true even at  $z \lesssim 1$  (except for the normalization of  $\Phi$ ): no mass-based constraints were employed at these redshifts (Sections 2.1, 2.2).

This is not to imply that such accuracy is unprecedented, or even uncommon: modern semi-analytic modeling can do better (e.g., Henriques et al. 2014; Lu et al. 2014). However, SAMs are far more complex and extensively tuned—often using  $\Phi$ —compared to our rather grossly (and independently) constrained ensemble of SFHs. The fact that our approach works as well as it does suggests either that the log-normal form is physically meaningful, or that  $\Phi$  is not strongly constraining in this context (see also Watson & Conroy 2013).

### 3.2. More on the Absence of Quenching

As mentioned, our model incorporates no explicit “quenching”; i.e., SFH discontinuities turning star-forming galaxies into non-star-forming ones. Because all model SFHs are continuous and smooth, the quiescent label is purely semantic; it is *not* an indication that a galaxy belongs to a qualitatively different population.

As shown in Figure 2, “quiescent” in our model really means “finished”: the SFHs of these galaxies are distinguished from their star-forming peers’ only by smaller  $(T_0, \tau)$  values, reflecting earlier, more rapid growth. This scenario appears compatible with the models of Hearin & Watson (2013, see below) and perhaps Wechsler et al. (2002), wherein halo *age* largely sets a galaxy’s eventual color/SFR or halo concentration.

This said, our results do not rule-out abrupt quenching events/scenarios, or fundamental bimodality in the galaxy population. They simply suggest that these phenomena are not necessary to reproduce the SFMS,  $\Phi$  or  $\Phi_Q$ , and the evolution of cosmic SFRD.

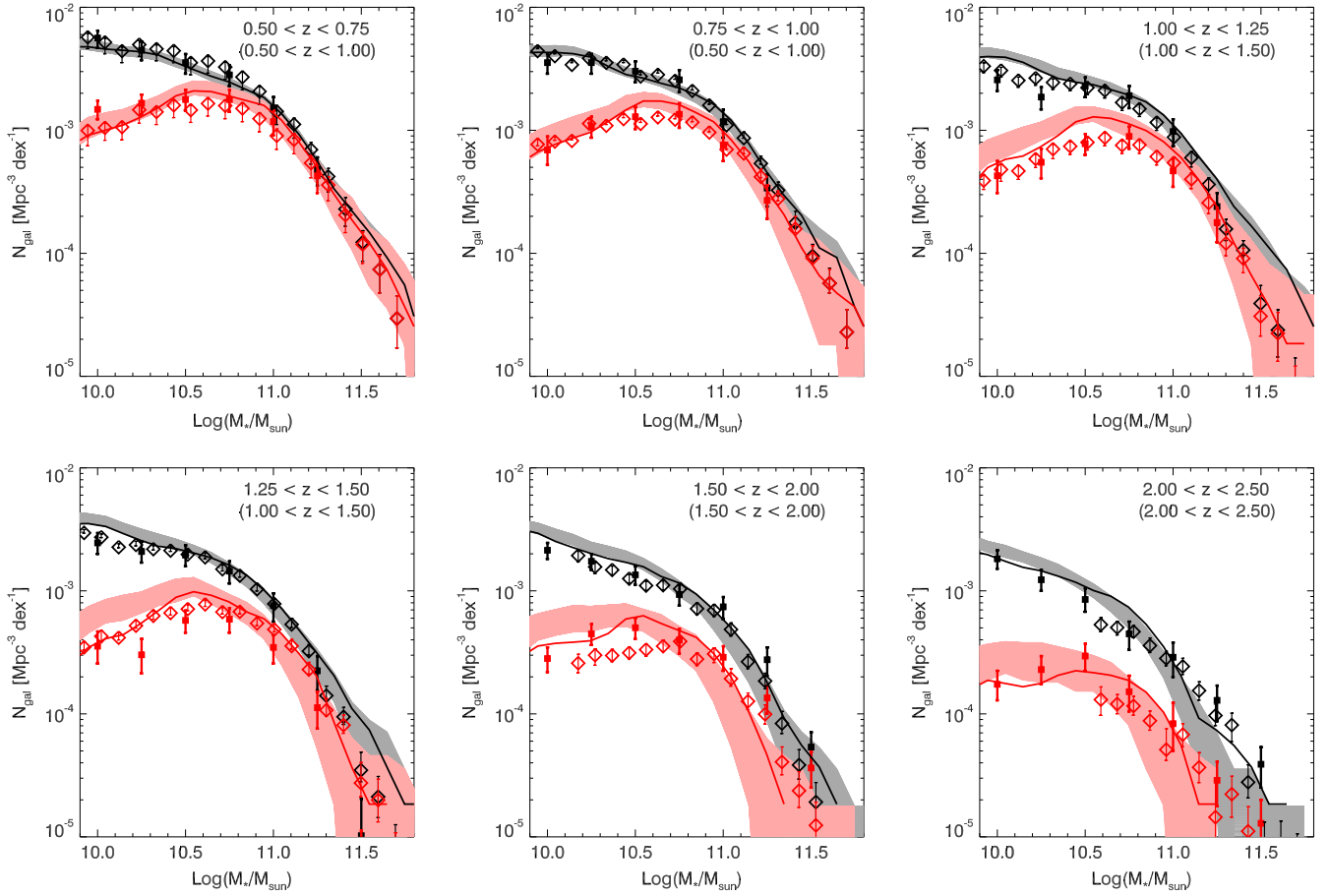


**Figure 1.** The evolution of  $\Phi$  and  $\Phi_Q$  since  $z \sim 2.5$ . Diamonds/squares show Muzzin et al. (2013) and Tomczak et al. (2014) data, respectively. Redshift binning matches the Tomczak et al. (2014) data; parentheses denote the coarser Muzzin et al. (2013) intervals from which those data were drawn. Shaded pink and gray bands are  $\Phi$  and  $\Phi_Q$ , respectively, predicted using the ensemble of log-normal SFHs from Gladders et al. (2013). Solid lines show results if mergers are neglected. Though no  $M_*$  information was used to constrain the models, the predicted evolution of the mass functions agrees remarkably well with the data, suggesting the log-normal SFH is consistent with real galaxy SFHs at the mass-bin level, and also that smooth, continuous SFHs can reproduce the observed evolution of the “quenched” population.

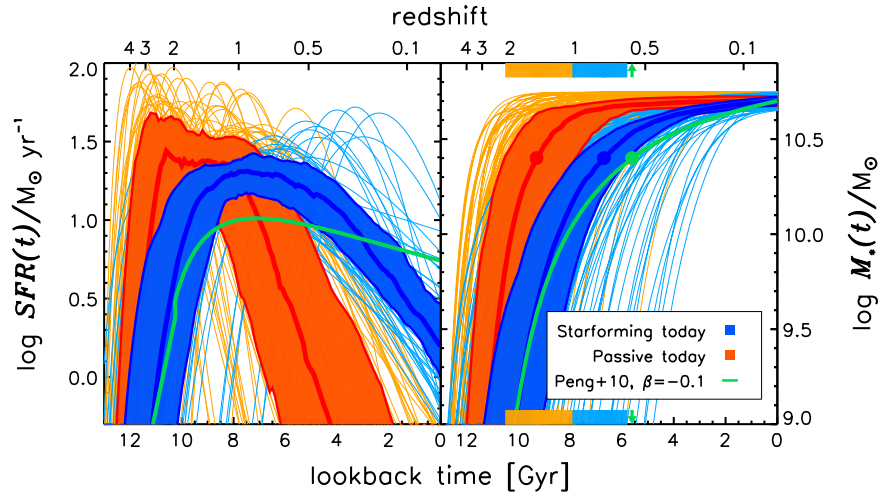


**Figure 2.** A comparison of G13 SFHs (left) and mass-growth curves (right) for today’s Milky Way–mass galaxies to the result of Peng et al. (2010; green curve). Turquoise/orange lines denote currently star-forming/quiescent G13 galaxies ( $sSFR \geq$  and  $< 10^{-11} \text{ yr}^{-1}$ , respectively); blue and red bands show 25%/75% spreads of these SFHs at fixed time. At right, turquoise/orange bars denote the 25%/75% range in half-mass times for the G13 SFHs; green arrows show that for the Peng et al. (2010) curve. These models paint different astrophysical pictures, but both appear capable of matching important metrics of galaxy evolution. Clearly, a key distinction is the prediction of a wide diversity of SFHs by the dispersion-based G13 model (e.g., a  $\sim 2$  Gyr inter-quartile range in half-mass times for MW analogs), which is difficult to reproduce from the “mean-based” perspective.

### 3.3. Environment

Our model incorporates no spatial information, so it cannot predict, e.g., trends in the quiescent fraction with environment. However, because our input data span a range of local densities, our results do encode such trends. Indeed, the previous section illuminates how our framework might reinterpret environment’s role: rather than quenching star formation, it might accelerate it, displacing  $(T_0, \tau)$  to lower values. Galaxy evolution in the largest, fastest-growing primordial overdensities—the progenitors of today’s passive-dominated groups and clusters—would thus be compressed, but not fundamentally divergent from that in lower-density regions.

Such a scenario would naturally interleave halo formation time, environmental density/group membership, the galaxy correlation function, and a system’s ultimate fate as quiescent or not. It thus implies a (strong) connection between  $(T_0, \tau)$ —i.e., galaxy age—and, for example, clustering strength. At present, our modeling procedure cannot elucidate the nature of that connection, but Hearin & Watson (2013), Oemler et al. (2013), Guglielmo et al. (2015) present compelling theoretical and empirical evidence that it—or something very similar—is in fact real.

### 3.4. Implications

At a minimum, the results above combined with those from G13 suggest that the log-normal parametrization is consistent with real galaxy SFHs to at least the level at which the SFMS,  $\Phi$  or  $\Phi_Q$ , and SFRD( $t$ ) are sensitive to them. However, because they show that these ensemble metrics—often modeled using the mean behavior of statistical quantities (e.g.,  $\langle \text{sSFR}(M_*, t) \rangle$ ; Peng et al. 2010)—can be reproduced using evolutionary tracks for individual galaxies, these results also reinforce the potential of “dispersion-based” approaches to assessing galaxy SFHs. We explore these issues in the next section.

## 4. DISCUSSION

We have shown—here and in G13—that a model composed solely of log-normal SFHs for individual galaxies is capable of matching three important ensemble observables related to galaxy evolution:

- (1) the cosmic SFRD (G13; by construction);
- (2) the SFMS at  $z \lesssim 2$  (G13);
- (3) the evolution of  $\Phi$  and  $\Phi_Q$  at  $z \lesssim 2.5$  (this paper).

We are not alone in this accomplishment, however. Others have approached SFRD( $t$ ),  $\Phi$ , the SFMS, and SFHs in a semi-empirical, (quasi-)holistic fashion (e.g., Peng et al. 2010; Behroozi et al. 2013; Moster et al. 2013; Kelson 2014; Lu et al. 2014). Not all were principally concerned with extracting SFHs (e.g., Peng et al. 2010), and not all attempted to match each of these “pillars” (e.g., Lu et al. 2014), but the results presented above and in these other works suggest that there are now many “good” descriptions of the data as far as SFHs are concerned.<sup>5</sup> So: have we identified an especially meaningful SFH form, or are the benchmark metrics simply (too) easy to reproduce? Can we determine which is the case?

<sup>5</sup> We recognize that many of these models are capable of matching additional data—such as the galaxy 2-point correlation function—that our model does not address.

### 4.1. Different Philosophies

To address these questions, we must first understand what distinguishes the aforementioned analyses (in the context of SFHs). Broadly, they fall into two categories: “mean-based” (Peng et al. 2010; Behroozi et al. 2013; Lu et al. 2014) and “dispersion-based” (G13; Kelson 2014).

The mean-based approaches use ensemble averages to infer the behavior of individual systems. They tend to center around a mapping between some “fundamental” quantity and  $\dot{M}_*(t)$ . This mapping can be the SFMS itself (Peng et al. 2010), or theoretical dark matter halo growth models combined with, e.g.,  $M_{\text{halo}}-M_*$  (Behroozi et al. 2013) relations. Regardless, since they are driven by statistical averages, their ability to assess *diversity* in SFHs at fixed  $(M_*, \text{SFR}, t)$  is limited by construction (Figure 2, green curve).

By contrast, the dispersion-based approaches (G13; Kelson 2014) entail no central mappings. They accommodate, for example, significant/arbitrary scatter in the SFMS, and so have great ability to capture diversity in SFHs (Figure 2, turquoise/orange curves; Figure 2 of Kelson 2014). However, this freedom is paid for by placing demands on the (nature of the) SFHs themselves: Kelson (2014) requires them to be governed by quasi-stochastic processes; we implicitly attribute physical importance to the log-normal form.

The crux of the issue is this: both mean-based and dispersion-based approaches have demonstrated significant potential in terms of their ability to match key metrics of galaxy evolution, but the way they view diversity—either in galaxy SFHs or as manifest by dispersion in statistical relations—are quite different. Addressing one question in particular will elucidate the relevance of either approach to real galaxy SFHs: To what extent did today’s equal-mass star-forming galaxies “grow up” together?

As shown by Muñoz & Peebles (2014), robust knowledge of the timescale encoded by the SFMS dispersion,  $\sigma_{\text{SFMS}}$ , is critical to answering this question.

### 4.2. What Is $\sigma_{\text{SFMS}}$ ?

Assuming it does not reflect observational errors,<sup>6</sup> there are three interpretations for  $\sigma_{\text{SFMS}}$ : (1) short-timescale ( $10^{\sim 7}$  yr) perturbations, (2) intermediate-timescale ( $10^{8-9.5}$  yr) variations, or (3) Hubble-timescale ( $10^{\sim 10}$  yr) differentiation. Muñoz & Peebles (2014) provide a good comparison/analysis of these scenarios. If (1) is the case, the mean-based approach is accurate: today’s Milky Way–mass star-forming galaxies mostly grew-up together. As such, we may have already identified the most critical astrophysics shaping SFHs (Peng et al. 2010; Behroozi et al. 2013). However, if (2) or especially (3) is the case, the dispersion-based approaches and their consequences must be examined more thoroughly: the mean history is a poor description of the real history of most MW-like galaxies, and critical astrophysics lies in what diversifies SFHs.

Because galaxy structure (generally) changes on timescales longer than the SFR, one way forward is a detailed morpho-structural study of equal-mass SFMS galaxies. If  $\sigma_{\text{SFMS}}$  reflects short “blips,” then there is essentially one way to reach a given  $(M_*, t)$  and still land on the SFMS. Hence, the mean-based

<sup>6</sup> Through detailed comparisons of SFRs obtained using different techniques, we are in the process of quantitatively demonstrating this to be true (A. Oemler et al. 2015, in preparation).

models suggest there should be little-to-no diversity in, e.g., bulge-to-total mass ratios for these galaxies. In the intermediate-timescale, quasi-stochastic model of Kelson (2014), there are many disparate paths to such an endpoint, suggesting a uniform structural mix. Finally, in the Hubble-timescale case of G13, the paths are numerous, but coherent. As such, that model predicts a trend in structural properties as a function of distance from the mean SFMS relation.

Many works now point to morphology/structure as as important to shaping the star formation histories (Salmi et al. 2012; Abramson et al. 2014) or pulling galaxies off it (Martig et al. 2009; Williams et al. 2010; Wuyts et al. 2011; Bluck et al. 2014; Lang et al. 2014; Omand et al. 2014). However, it is still unclear if/how it distinguishes galaxies *on* it. Hence, it may relate to “quenching” (consistent with mean-based models) *or* “diversification” (as implied by dispersion-based models). The goal is to determine which is the case.

## 5. CONCLUSION

We have shown that a model consisting of a broad continuum of individual, log-normal star formation histories and entailing no explicit quenching prescription matches the evolution of the total and quiescent stellar mass functions at  $z \lesssim 2.5$ . Constrained at  $z \lesssim 1$ , it also reproduces the observed  $z \approx 2$  SFR– $M_*$  relation and is fully consistent with the evolution of the cosmic SFR density at  $z \leq 8$  (Gladders et al. 2013). In terms of providing a viable description of SFHs, these achievements make our model competitive with those based on mean statistical relations. However, our results also stress the fact that key observational “pillars” of galaxy evolution can accommodate great diversity in individual growth histories, something missed using a mean-based modeling approach. To determine the physical import of this difference in perspective, we suggest that a robust assessment of the true diversity in star formation histories—especially of today’s star-forming galaxies—is key. Measurements of the size and timescale associated with dispersion in SFR( $M_*$ ) will substantially aid this effort.

L.E.A. thanks Daniel Kelson for his patience and Doug Watson, Avishai Dekel, Nir Mandelker, and the referee for their thoughtful and helpful responses to our original draft. He also acknowledges generous support from the inaugural James Cronin Fellowship.

## REFERENCES

- Abramson, L. E., Kelson, D. D., Dressler, A., et al. 2014, *ApJL*, **785**, L36  
 Ball, N. M., Loveday, J., Brunner, R. J., Baldry, I. K., & Brinkmann, J. 2006, *MNRAS*, **373**, 845  
 Behroozi, P. S., Wechsler, R. H., & Conroy, C. 2013, *ApJ*, **770**, 57  
 Bluck, A. F. L., Mendel, J. T., Ellison, S. L., et al. 2014, *MNRAS*, **441**, 599  
 Brinchmann, J., Charlot, S., White, S. D. M., et al. 2004, *MNRAS*, **351**, 1151  
 Calvi, R., Poggianti, B. M., & Vulcani, B. 2011, *MNRAS*, **416**, 727  
 Cucciati, O., Tresse, L., Ilbert, O., et al. 2012, *A&A*, **539**, A31  
 Gladders, M. D., Oemler, A., Dressler, A., et al. 2013, *ApJ*, **770**, 64  
 Guglielmo, Poggianti, Moretti, et al. 2015, *MNRAS*, submitted  
 Hearin, A. P., & Watson, D. F. 2013, *MNRAS*, **435**, 1313  
 Henriques, B., White, S., Thomas, P., et al. 2014, arXiv:1410.0365  
 Kauffmann, G., Heckman, T. M., White, S. D. M., et al. 2003, *MNRAS*, **341**, 33  
 Kelson, D. D. 2014, arXiv:1406.5191  
 Lang, P., Wuyts, S., Somerville, R., et al. 2014, *ApJ*, **788**, 11  
 Lu, Z., Mo, H. J., Lu, Y., et al. 2014, arXiv:1406.5048  
 Madau, P., & Dickinson, M. 2014, *ARA&A*, **52**, 415  
 Martig, M., Bournaud, F., Teyssier, R., & Dekel, A. 2009, *ApJ*, **707**, 250  
 Moster, B. P., Naab, T., & White, S. D. M. 2013, *MNRAS*, **428**, 3121  
 Moustakas, J., Coil, A. L., Aird, J., et al. 2013, *ApJ*, **767**, 50  
 Muñoz, J. A., & Peeples, M. S. 2014, arXiv:1404.1915  
 Muzzin, A., Marchesini, D., Stefanon, M., et al. 2013, *ApJ*, **777**, 18  
 Noeske, K. G., Weiner, B. J., Faber, S. M., et al. 2007, *ApJL*, **660**, L43  
 Oemler, A., Jr, Dressler, A., Gladders, M. G., et al. 2013, *ApJ*, **770**, 63  
 Omand, C. M. B., Balogh, M. L., & Poggianti, B. M. 2014, *MNRAS*, **440**, 843  
 Peng, Y.-j., Lilly, S. J., Kovač, K., et al. 2010, *ApJ*, **721**, 193  
 Salmi, F., Daddi, E., Elbaz, D., et al. 2012, *ApJL*, **754**, L14  
 Salmon, B., Papovich, C., Finkelstein, S. L., et al. 2014, arXiv:1407.6012  
 Tomczak, A. R., Quadri, R. F., Tran, K.-V. H., et al. 2014, *ApJ*, **783**, 85  
 Watson, D. F., & Conroy, C. 2013, *ApJ*, **772**, 139  
 Wechsler, R. H., Bullock, J. S., Primack, J. R., Kravtsov, A. V., & Dekel, A. 2002, *ApJ*, **568**, 52  
 Williams, R. J., Quadri, R. F., Franx, M., et al. 2010, *ApJ*, **713**, 738  
 Wuyts, S., Förster Schreiber, N. M., van der Wel, A., et al. 2011, *ApJ*, **742**, 96  
 York, D. G., Adelman, J., Anderson, J. E., Jr., et al. 2000, *AJ*, **120**, 1579